Supplemental Figure 1

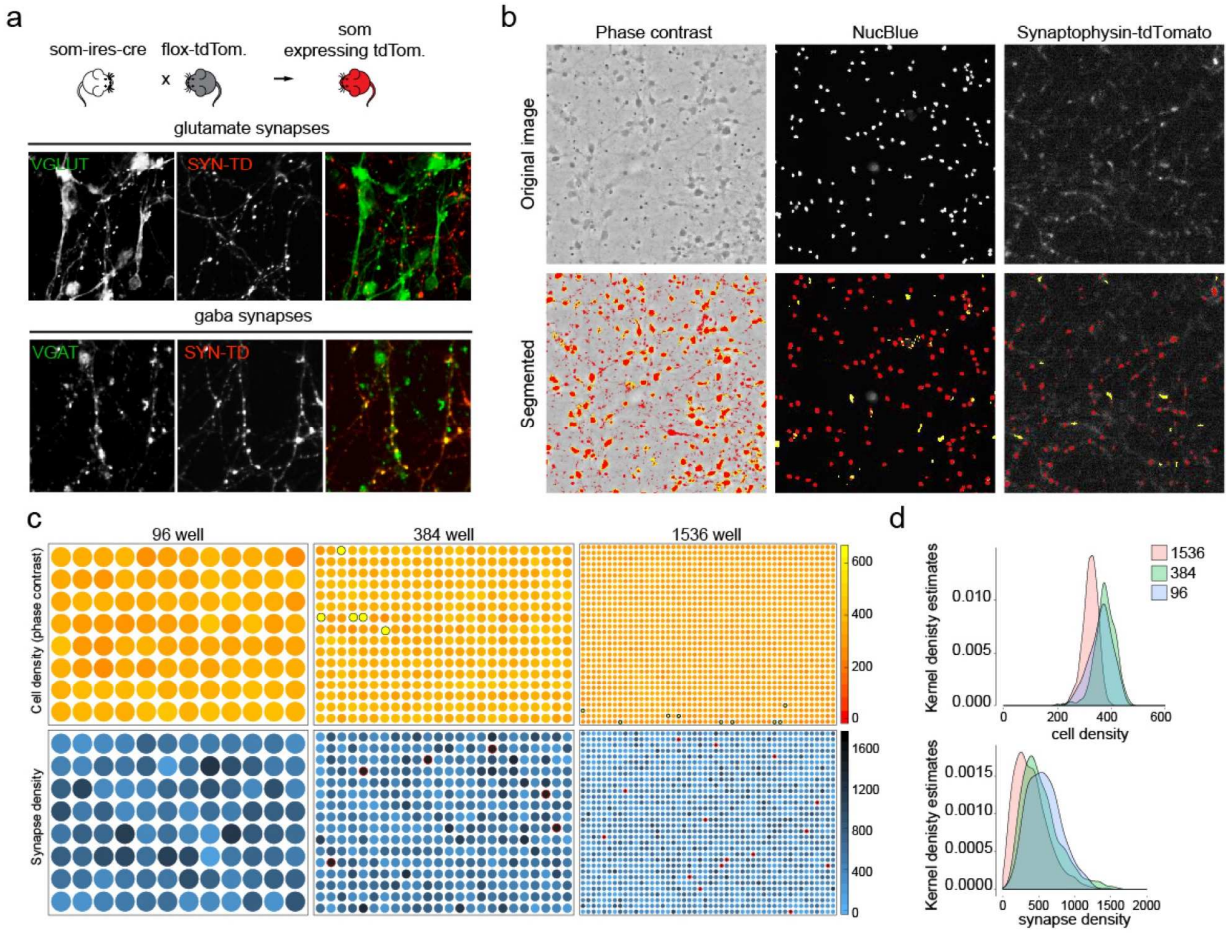

Supplemental Figure 1. Platform flexibility and scalability. (a) Breeding strategy for presynapse reporter expression restricted to a subset of GABAergic neurons. Immunostaining (anti-Vglut for excitatory synapses; anti-Vgat for inhibitory synapses) of primary neurons cultured from these mice show selective labeling of a subset of GABAergic presynapses. **(b)** Automated segmentation and quantification of cells for phase contrast, NucBlue and presynaptic terminals at DIV7 (red puncta). Structure that fail to meet criteria are filtered out (outside of yellow border for phase contrast images and yellow puncta for nuclear and synapse segmentation). NucBlue and Syn-TD images are shown at different scales due to the different size of each segmented structure. **(c)** Heatmap of raw cell and synapse densities with outlier wells circled in black (cell) and red (synapses). **(d)** Cell and synapse density distribution displayed on a probability density plots for 3 formats: 96, 384, 1536-well plates at DIV7. DIV: days in vitro.

Supplemental Figure 2

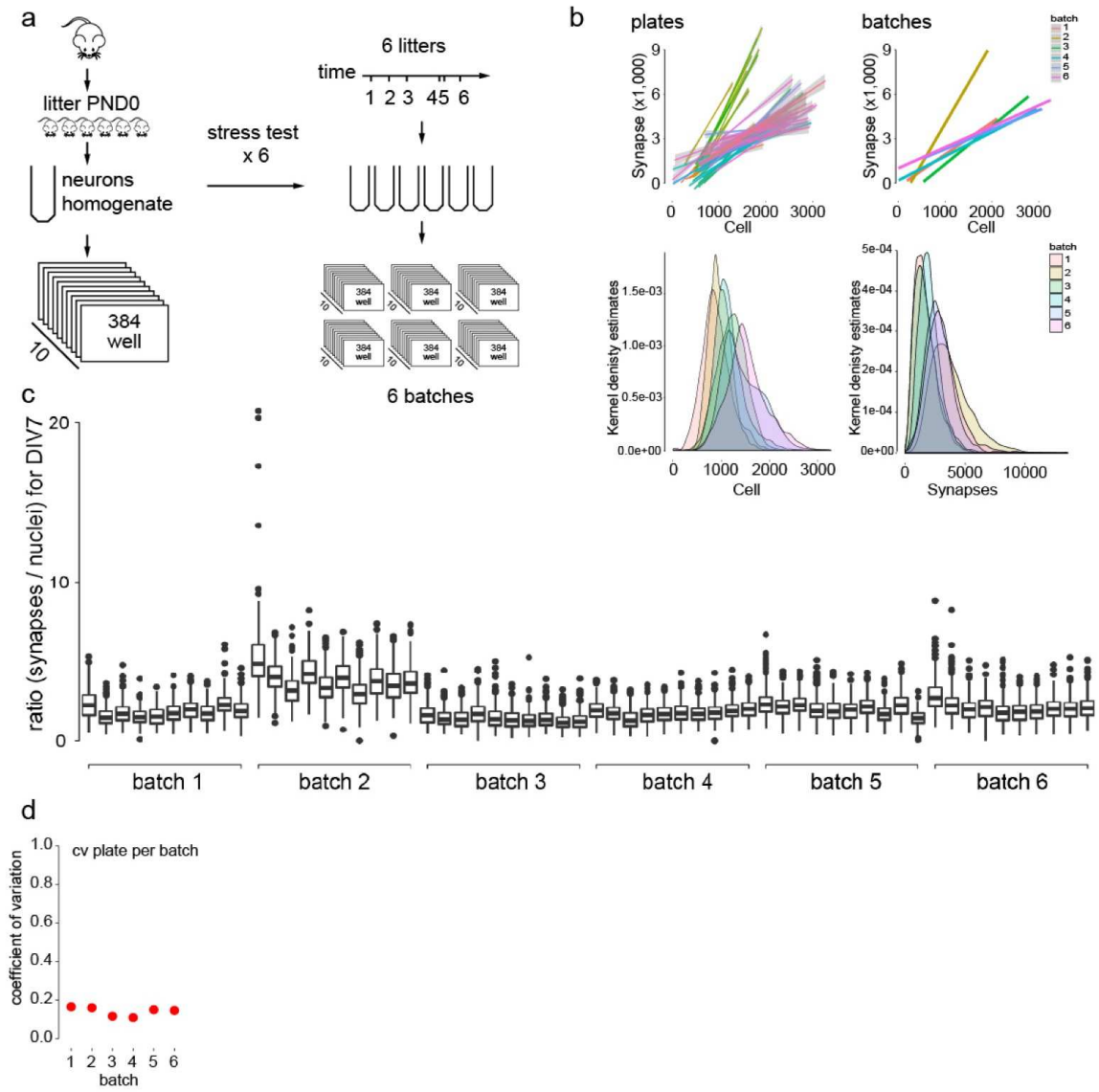

Supplemental Figure 2. Reliability of primary neurons cultured using automated procedures. (a) Strategy for stress test to generate ten, 384-well plates from 1 litter replicated across six batches over a three-week period. **(b)** Relationship between synapse and cell number at DIV7 for all plates (upper left) and the six batches (upper right). *lower panels,* Probability density for cell and synapse numbers across the 6 batches derived from nuclear and synapse segmentation. **(c)** Number of synapses per nuclei visualized as boxplot per plate. Median are presented within boxes for the 75th and 25th quantiles for which +/- 1.5 times the interquartile values are displayed as vertical bars, dots represents outliers. **(d)** Grand average of the coefficient of variation for each ten-plate batch.

Supplemental Figure 3

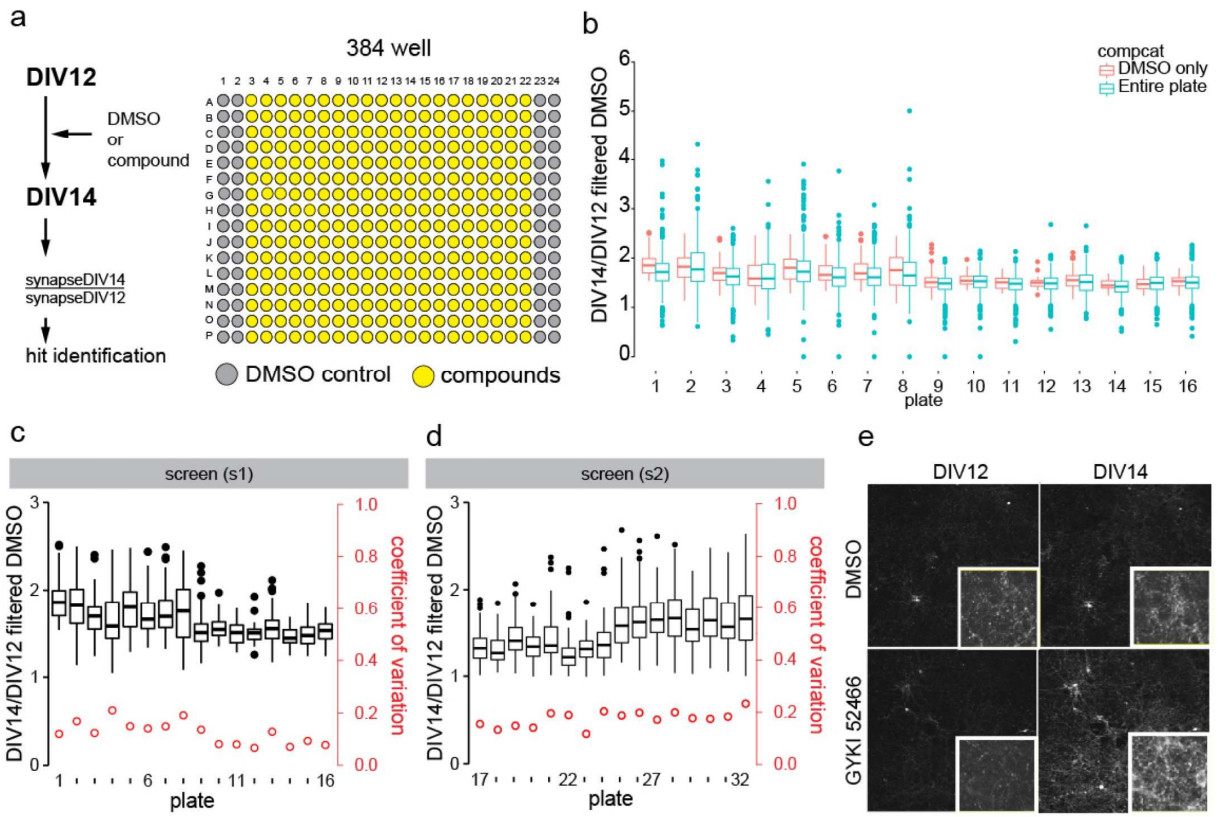

Supplemental Figure 3. Variability and normalization for low and high throughput screening of LOPAC library compounds in a synaptogenesis assay. (a) Screening strategy for functional synapse assay (384w format) and location of controls and compounds during LOPAC screening for screen s1 and s2. **(b)** Comparison of synapse ratio and normalization strategy in the screen *s1*. Distribution of ratios for DMSO control and entire plate. The lower median observed for the entire plate compare to DMSO control suggest that normalizing to control will lead to lower false positive rate. Normalization to the DMSO control or normalization with z-score using the entire plate under the assumption that most compounds are inactive resulted in similar putative hit list. **(c)** Synaptogenesis occurring over 2 days in the DMSO control well and their respective coefficient of variation in the screen (s1) DMSO control outliers that were 3 standard deviation from the mean were removed from the analysis. **(d)** Analysis as in **a** for the screen s2 performed in uHTS environment. **(e)** Synaptophysin-TdTomato expression at DIV12 and DIV14 for DMSO and the replicated hit GYKI52466. (b-d) Boxplot representing median within boxes for the 75th and 25th quantiles for which +/- 1.5 times the interquartile values are displayed as vertical bars, dots represent outliers.

Supplemental Figure 4

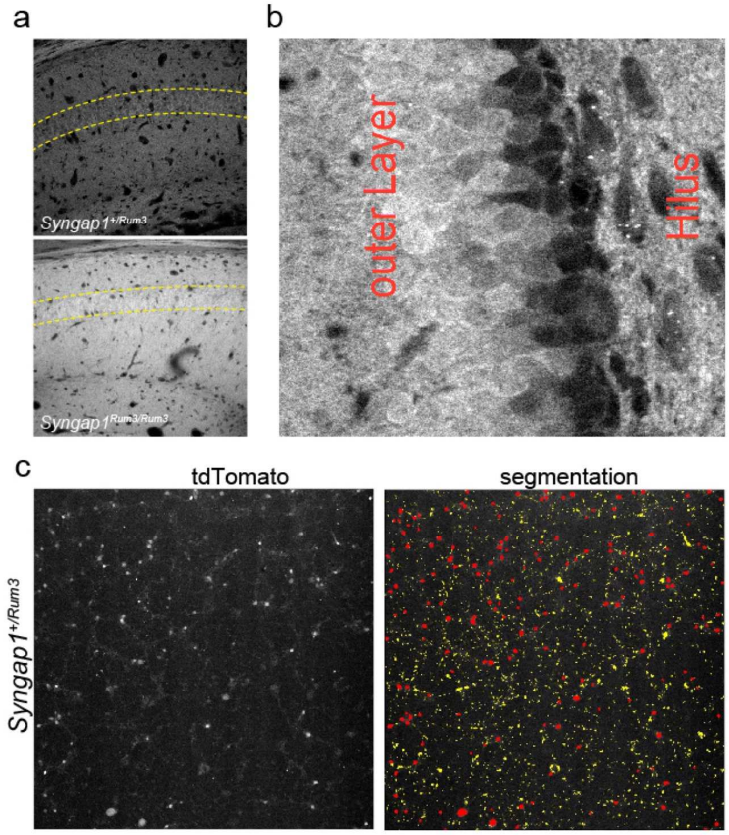

Supplemental Figure 4. Characterization of a *Syngap1* reporter mouse. (a) PND21 Heterozygous or Homozygous Rum3 knock-in mice were fixed, sectioned, mounted and then imaged on a confocal microscope. Images depict endogenous tdTomato fluorescence in each genotype; imaging parameters were identical in each case. **(b)** Confocal image of the dentate gyrus of a Heterozygous Rum3 mouse sectioned at PND21. Newborn neurons in the inner molecular layer have lower levels of endogenous tdTomato expression. **(c)** A segmented image from a plate used in the Rum3 pilot screen. Red segmented objects denote tdTomato+ soma and yellow objects were structures rejected by the analysis algorithm. The assay endpoint was calculated from the average intensity of all segmented tdTomato soma in each assay well.

Supplemental Table 1

screen (s1)	
By plate to control normalization	By plate z-score normalization
Anisotropine methyl bromide	AS-252424
AS-252424	Carbetapentane citrate
Carbetapentane citrate	Cinnarizine
Cinnarizine	HI-TOPK-032
Dihydroergotamine methanesulfonate	Anisotropine methyl bromide
Fluphenazine dihydrochloride	Dihydroergotamine methanesulfonate
GYKI 52466 hydrochloride	Fluphenazine dihydrochloride
HI-TOPK-032	**GYKI 52466 hydrochloride**
Hydroxylamine hydrochloride	Hydroxylamine hydrochloride
	Wiskostatin

Supplemental Table 2

screen (s2 - uHTS)	
By plate to control normalization	By plate z-score normalization
Atreleuton	8-Cyclopentyl-1,3-dipropylxanthine
8-Cyclopentyl-1,3-dipropylxanthine	**GYKI 52466 hydrochloride**
GYKI 52466 hydrochloride	Hydralazine hydrochloride
Hydralazine hydrochloride	Iofetamine hydrochloride
Iofetamine hydrochloride	Methoctramine tetrahydrochloride
Methoctramine tetrahydrochloride	Phenamil methanesulfonate
Phenamil methanesulfonate	Pirenperone
Ranolazine dihydrochloride	Ranolazine dihydrochloride
Ro 41-0960	Ro 41-0960
SIB 1893	SIB 1893
	Tetrabenazine
	Tetraethylthiuram disulfide

Supplemental Table 3

By plate to control normalization	By plate z-score normalization
AC-93253 iodide	AC-93253 iodide
ML 10302	ML 10302
Genipin	Genipin
HI-TOPK-032	HI-TOPK-032
BIO	BIO
Idarubicin	Idarubicin
Sulindac sulfone	NSC 95397
NSC 95397	Sulindac sulfone
Reserpine	Reserpine
7-Cyclopentyl-5-(4-phenoxy)phenyl-7H-pyrrolo[2,3-d]pyrimidin-4-ylamine	7-Cyclopentyl-5-(4-phenoxy)phenyl-7H-pyrrolo[2,3-d]pyrimidin-4-ylamine
Flupirtine maleate	
SB 216763	
U-74389G maleate	
Phenylephrine hydrochloride	
L2-b	
LE 300	
AMN082	
9-Amino-1,2,3,4-tetrahydroacridine hydrochloride	
Doxepin hydrochloride	